IV International Conference on Computational Methods for Coupled Problems in Science and Engineering
COUPLED PROBLEMS 2011
M. Papadrakakis, E. Oñate and B. Schrefler (Eds)

SUBLOADING SURFACE PLASTICITY MODEL ALGORITHM FOR 3D SUBSIDENCE ANALYSES ABOVE GAS RESERVOIRS

VALENTINA A. SALOMONI*, RICCARDO L. FINCATO*

* Department of Structural and Transportation Engineering
Faculty of Engineering, University of Padua
Via F.Marzolo, 9 – 35131 Padua, Italy
e-mail: salomoni@dic.unipd.it, fincato@dic.unipd.it, www.dic.unipd.it

Key words: Subsidence, Plasticity, Subloading surface, Environmental impact, Gas recovery.

Abstract. The coupled hydro-mechanical state in soils coming from consolidation/subsidence processes and undergoing plasticity phenomena is here evaluated by means of the subloading surface model. The most important feature of this theory is the abolition of the distinction between the elastic and plastic domain, as it happens in conventional elastoplastic models. This means that plastic deformations are generated whenever there is a change in stress and a smoother elasto-plastic transition is produced.The plasticity algorithm has been implemented in the PLASCON3D FE code (on the basis of a previous 2D version), coupling hydro-(thermo)-mechanical fields within a saturated porous medium (locally partially saturated at reservoir level due to the possible presence of a gas phase) subjected to external loads and water/gas withdrawals from deep layers (aquifers/reservoirs). The 3D model has been first calibrated and validated against examples taken from literature, and then subsidence analyses at regional scales due to gas extractions have been developed to predict the evolution of settlements and pore pressure in soils for long-term scenarios.

1 INTRODUCTION

Surface subsidence due to withdrawal of underground fluids occurs in many parts of the world, see for instance the case book of Poland [1]. Underground fluids involved are either water from superficial aquifers or gas and oil from usually deeper reservoirs. Such surface settlement is a particular threat if it is experienced in low lying areas, close to the sea, e.g. Groningen in the Netherlands (gas), Venice (water) and Ravenna (water and gas) in Italy, Wilmington (oil) in the USA. Surface subsidence of this kind is almost exclusively understood in terms of drop of pressure in the aquifers or in the reservoir: i.e. withdrawal of these underground fluids results in a reduction of their pressure downhole; this in turn increases the part of the overburden carried by the skeleton of the reservoir rocks causing compaction. The compaction manifests itself, through deformation of the overlying strata, as surface settlement.

In case of a single fluid (water) involved, compaction can easily be explained by the principle of Terzaghi [2] which states that the compression of a porous medium is controlled by changes of effective stresses, i.e. variations of the difference between total stresses and the

pressure of the fluid in the pores. However, when more fluids are involved or more phases of the same fluid, the Terzaghi traditional expression of effective stress alone is not sufficient to completely justify measured compaction and the concepts of unsaturated soil mechanics with appropriate stress measures and elastoplasticity concepts are needed. Drop of reservoir pressure is not the only mechanism leading to reservoir compaction and suction effects must also be accounted for at least for some types of extracted fluids and some reservoir rocks.

It is then proposed in [3-5] that capillary effects and structural collapse can not be ruled out as significant factors in the development of subsidence occurring above gas fields. These phenomena seem to provide sound explanations for continuing surface settlements when reservoir pore pressures stabilise and for additional settlements occurring even after the end of gas production. However, it is to be said that for the investigated area here considered, undergoing subsidence, there is no direct experimental evidence on samples from the field to show the key effect of capillarity on subsidence itself and hence any additional consideration could be largely speculative with many assumptions that are not justified enough.

Again, the discussion about the contribution of capillary effects when performing reservoir compaction and subsidence analyses at regional scale is out of scope for the present paper. The idea is to make use of unconventional plasticity [6] by means of the subloading surface model [7-11] for predicting softening behaviour of soil as well as reducing computational efforts when performing fully coupled hydro-mechanical subsidence analyses in three-dimensional domains [12], as demonstrated below. The reader is referred to [13] for discussions about modelling strain-softening from the computational point of view.

2 THE PROBLEM OF SUBSIDENCE ABOVE GAS RESERVOIRS

The particular subsidence problem solved here is first briefly summed up as follows [14-18]. It is supposed that there are several gas reservoirs at different levels, and some of the reservoirs have an edge aquifer. It is further assumed that in each respective domain there is only one fluid: water in the aquifers and gas in the reservoirs. The gas, upon exploitation of the reservoirs, may be substituted by encroaching water, which comes from the edge aquifers and from possible leaky aquitards. Capillary effects due to the simultaneous presence of gas and water in the reservoirs are not accounted for, as previously explained.

Under these assumptions the following balance equations can be written, where the chosen macroscopic field variables are displacements **u** and water pressure p_w.

Linear momentum balance equation for the mixture solid + water or solid + gas

$$\nabla\dot{\boldsymbol{\sigma}} = \mathbf{0} \tag{1}$$

where $\boldsymbol{\sigma}$ is the total stress tensor; no variable body forces are accounted for.

An averaged density of the mixture of the form

$$\rho = (1-\phi)\rho_S + \phi\rho_\pi \qquad \pi = \text{w (water) or g (gas), s = solid} \tag{2}$$

ϕ being the porosity, is assumed in the following.

Flow conservation equation for the aquifers and aquitards

$$-\nabla\left\{\frac{\mathbf{k}}{\mu}\nabla\left(p_w + \rho_w g h\right)\right\} + \left(\mathbf{m}^T - \frac{\mathbf{m}^T\mathbf{D}_T}{3K_s}\right)\frac{\partial\boldsymbol{\varepsilon}}{\partial t} + \left[\frac{(1-\phi)}{K_s} + \frac{\phi}{K_w} - \frac{1}{(3K_s)^2}\mathbf{m}^T\mathbf{D}_T\mathbf{m}\right]\frac{\partial p_w}{\partial t} = 0 \tag{3}$$

where **m** is a vector with components equal to unity for the normal stress components and zero for the shear stress components, K_w the bulk modulus, K_s the averaged bulk modulus of the solid grains, k the absolute permeability matrix of the medium, $\mathbf{D}_T$ the tangent matrix, **ε** the total strain of the skeleton, μ the dynamic viscosity of water.

Instead of writing a similar mass balance equation as Eq. (3) for the gaseous phase, we consider its integral form for the whole reservoir volume. This is valid if the reservoir volume is small compared to the analysed cross section and its thickness is small compared to the depth of burial [15, 16, 18, 19]. The conservation equation assumes hence the form of a

Material balance equation for the reservoir

$$GB_{gi} = (G - G_p)B_g + W_e - W_p B_w \tag{4}$$

where G is the initial free gas in place, B_g the gas formation volume factor, B_w the water formation volume factor, G_p the cumulative gas production, W_p the cumulative water production and W_e the influx from the adjacent aquifer and from leaky aquitards; the index i denotes initial conditions. Its incremental form can be found in [13].

The model is completed by the constitutive relation for solid mechanical behaviour relating the effective stress **σ´** and the adopted strain measure. In general, for small displacement gradients, it can be written as

$$\dot{\boldsymbol{\sigma}}' = \mathbf{E}(\dot{\boldsymbol{\varepsilon}} - \dot{\boldsymbol{\varepsilon}}^p) \tag{5}$$

$\dot{\boldsymbol{\varepsilon}}^p$ being the plastic strain rate, and **E** the fourth order elasticity tensor.

3 MODELLING PLASTICITY – THE SUBLOADING SURFACE MODEL

The subloading surface model is a particular elasto-plastic model falling within the framework of unconventional elastoplasticity [6], an extended elastoplasticity theory such that the interior of the yield surface is not a purely elastic domain, but rather a plastic deformation is induced by the rate of stress inside the yield surface [7-11]. Its main features are briefly recalled here.

In the subloading surface model the conventional yield surface is renamed the normal yield surface, since its interior is not regarded as a purely elastic domain. The plastic deformation develops gradually as the stress approaches the normal yield surface, exhibiting a smooth elastic-plastic transition. Thus the subloading surface model fulfils the smoothness condition [11, 20-22], which is defined as the stress rate-strain rate relation (or the stiffness tensor) changing continuously for a continuous change of stress rate. Strain accumulation is predicted for a cyclic loading with an arbitrary stress amplitude, where the magnitude of accumulated strain depends continuously on the stress amplitude because of the fulfillment of the smoothness condition. Inelastic deformation occurs immediately when the stress point once again moves outward the current yield surface. Zero diameter yield surface bounding surface models, nested surface models, and subloading models have this attribute, but do not display any purely elastic response [6].

A subloading surface is also introduced (together with the normal yield one), which always passes through the current stress point σ and keeps a shape similar to that of the normal yield surface and a similar orientation with respect to the origin of stress space, i.e. $\boldsymbol{\sigma} = \mathbf{0}$.

The ratio of similarity is named normal yield ratio and governs the approach of the

subloading surface to the normal one, i.e. if R = 0 the subloading surface is a point coinciding with the origin of the stress space, whereas 0 < R < 1 represents the subyield state and with R = 1 the stress lies directly on the normal surface.

The subloading surface can be described by the scalar-valued tensor function

$$f(\boldsymbol{\sigma}) = RF(H) \tag{6}$$

where the scalar H is the isotropic hardening/softening variable; in agreement with [10] the normal yield surface takes e.g. the form

$$F = F_0 \exp\left(\frac{H}{\rho'-\gamma}\right) \tag{7}$$

in which F_0 is the initial value of F, ρ' and γ the slopes of the normal consolidation and swelling curves respectively in $\ln\upsilon$-$\ln p$ space (υ being the specific volume and $p = -\mathrm{tr}(\boldsymbol{\sigma})/3$).

The extended consistency condition for the subloading surface is obtained by differentiating Eq. (6), which leads to

$$\mathrm{tr}\left(\frac{\partial f(\boldsymbol{\sigma})}{\partial \boldsymbol{\sigma}}\dot{\boldsymbol{\sigma}}\right) = \dot{R}F + RF'\dot{H} \tag{8}$$

together with considering the evolution rule of the normal yield ratio, given by

$$\dot{R} = U\left\|\dot{\boldsymbol{\varepsilon}}^{p}\right\| \quad \text{for} \quad \dot{\boldsymbol{\varepsilon}}^{p} \neq \mathbf{0} \tag{9}$$

where $\dot{\boldsymbol{\sigma}}$ is the proper objective co-rotational stress rate, $\dot{\boldsymbol{\varepsilon}}^{e} = \mathbf{E}^{-1}\dot{\boldsymbol{\sigma}}$, and U is a monotonically decreasing function of R satisfying the condition

$$\begin{cases} U = +\infty & \text{for} \quad R = 0 \\ U = 0 & \text{for} \quad R = 1 \\ (U < 0 & \text{for} \quad R > 1) \end{cases} \tag{10}$$

The associated flow rule is assumed as

$$\dot{\boldsymbol{\varepsilon}}^{p} = \overline{\lambda}\,\overline{\mathbf{N}} \tag{11}$$

where $\overline{\lambda}$ is the positive proportional factor representing the increment of plastic deformation along the direction given by the normalized outward normal of the subloading surface $\overline{\mathbf{N}}$

$$\overline{\lambda} = \frac{\mathrm{tr}\,(\overline{\mathbf{N}}\dot{\boldsymbol{\sigma}})}{\overline{M}^{p}} \tag{12}$$

$$\overline{\mathbf{N}} \equiv \frac{\partial f(\boldsymbol{\sigma})}{\partial \boldsymbol{\sigma}} \Bigg/ \left\|\frac{\partial f(\boldsymbol{\sigma})}{\partial \boldsymbol{\sigma}}\right\| \tag{13}$$

being $\overline{M}^{p}$ the plastic modulus.

The loading criterion is finally given [22, 23]

$$\begin{cases} \dot{\boldsymbol{\varepsilon}}^{p} \neq \mathbf{0}: & \mathrm{tr}\,(\overline{\mathbf{N}}\mathbf{E}\dot{\boldsymbol{\varepsilon}}) > 0 \\ \dot{\boldsymbol{\varepsilon}}^{p} = \mathbf{0}: & \mathrm{tr}\,(\overline{\mathbf{N}}\mathbf{E}\dot{\boldsymbol{\varepsilon}}) \leq 0 \end{cases} \tag{14}$$

For additional details, see [13].

4 APPLICATION CASE: 3D SUBSIDENCE ANALYSIS ON REGIONAL SCALE

Surface subsidence due to extraction of underground fluids (water, hydrocarbons) plays an important role in reservoir engineering. For decades a great deal of attention has been directed towards modelling this phenomenon, also because it affects historical cities, like Venice and Ravenna in Italy [3-5, 15, 16, 18, 24-25]. Subsidence analyses are computationally intensive by involving problems of regional scale and very long time spans: e.g. in the case of the Groningen gas field, subsidence predictions for the year 2050 have been made from the year 1973 on. The subsidence surfaces have been obtained with different models and codes, e.g. in [26] with ECLIPSE [27]; in [25] with a quasi three-dimensional hydrologic model and a three-dimensional uncoupled structural model and in [9, 18] with a fully coupled consolidation model.

Apart from exceptions (as e.g. in [9]), three-dimensional subsidence models have assumed a linear elastic response for the solid skeleton and not much has been done for modelling possible interactions in case several reservoirs at different levels are distributed over a large area, as it is the case of the Northern Adriatic region, Italy [28] (**Figure 1**). Here the pools' depth of burial ranges between 900 and 4000 m and the horizontal area involved is about 19000 Km^2. In addition, the different pools are not scheduled to be put in production at the same time [30], which complicates the situation further.

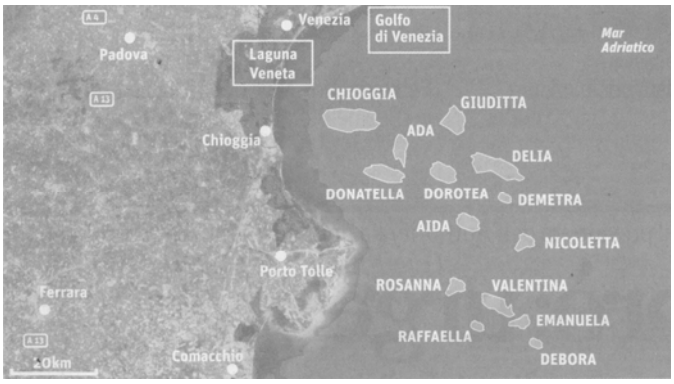

Figure 1: Location of gas pools in the Northern Adriatic Sea [29].

At present, creep, plasticity [28] and capillary effects [3-5] are envisaged among the possible processes yielding a retarded sinking over the reservoir; as already explained before, the choice here is to refer to an unconventional elastoplastic model, also being its potentialities independent on the specific application case treated here.

The effects of the exploitation of four of the gas reservoirs shown in **Figure 1**, located at three different depths and undergoing different production histories [30], are here analysed; the region covers an area of 40×40 km^2 and has a depth of 1300 m; it is discretized by about 500 20-node isoparametric elements (additional results, not reported here for sake of brevity, refer to 980 and 2940 elements as well). Free flux on the horizontal and vertical boundaries of the investigated area is assumed. The main material parameters are shown in **Table 1** [16, 30]; the grains are assumed to be incompressible and the clayey layers to behave in agreement with the subloading surface model when accounting for plasticity effects. The geomechanical data have been obtained through analysis of master-logs at our disposal, which are

representative of the investigated area, whereas the plastic variables have been taken from the previous examples, appropriately scaled to take into account the effect of depth.

Table 1: Material data for subsidence analysis

Soil stratum #	**E** [MPa]	ν	$\mathbf{k_i}$ [m/day]	**Depths [m]**
1	$1.13 \cdot 10^4$	0.17	0.2208	1300÷1254
2	$1.00 \cdot 10^4$	0.17	$0.865 \cdot 10^{-4}$	1300÷1254
3 & Reservoir # 1	$1.13 \cdot 10^4$	0.17	0.2208	1300÷1254
4	$1.00 \cdot 10^4$	0.17	$0.865 \cdot 10^{-4}$	1300÷1254 & 1300÷1070
5, 7, 9	$1.14 \cdot 10^4$	0.30	0.7985	1254÷1070
6, 8, 10	$0.322 \cdot 10^4$	0.38	$0.865 \cdot 10^{-4}$	1254÷1070
11 & Reservoir # 4	$1.14 \cdot 10^4$	0.30	0.7985	1070÷1027
12	$0.322 \cdot 10^4$	0.38	$0.865 \cdot 10^{-4}$	1027÷860
13 & Reservoirs # 2, 3	$0.898 \cdot 10^4$	0.15	0.9752	860÷848
14	$0.555 \cdot 10^4$	0.37	$0.865 \cdot 10^{-4}$	848÷600
15	$0.224 \cdot 10^4$	0.39	$0.865 \cdot 10^{-4}$	600÷0

As evidenced by **Table 1** and **Figure 2**, some planimetric variability for the soil strata has been additionally introduced just to be closer to the real configuration of the subsoil, e.g. considering the available seismic section of [30]; so 7 *macro-levels* are present, including 15 different soil strata. The horizontal projection of the investigated pools can be seen in **Figure 3**, together with the mean radius of their productive levels. The exploitation points (wells) are assumed to be equally distributed above each reservoir such as to allow for the assumption of a constant drop of pressure inside it. The pressure histories (**Figure 4**), obtained from previous reservoir simulators (starting from available gas production records developing in 10 years) are applied as boundary conditions to the nodes of each pool. A computationally more expensive alternative would be to apply the outflow given from the production schedule (if available).

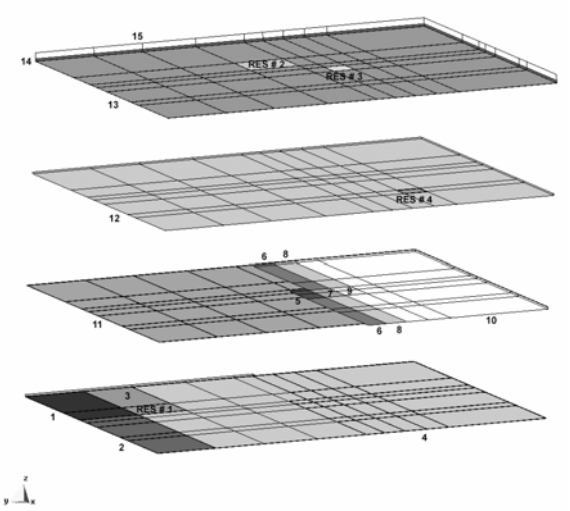

Figure 2: Schematic representation of the soil strata distribution: macro-levels are superimposed from surface (top) to bottom (see **Table 1**).

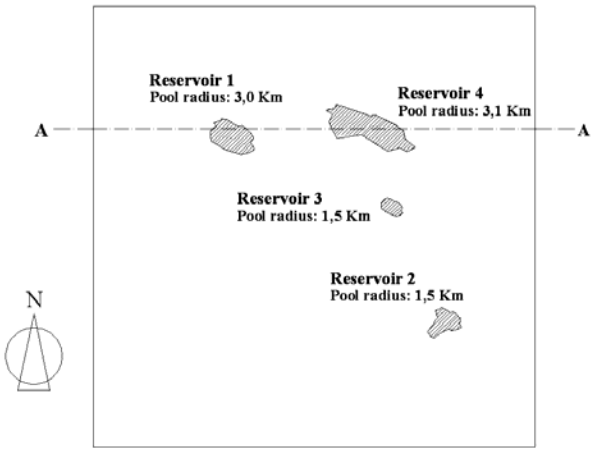

Figure 3: Horizontal projection of the investigated reservoirs for subsidence analysis.

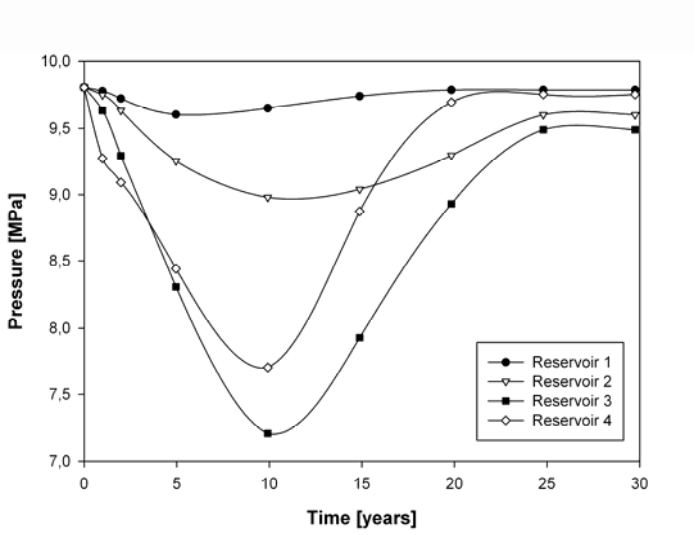

Figure 4: Reservoirs' pressure histories.

The analysis has been pushed up to 30 years from the beginning of exploitations, when a general pressure recovery has already been attained (**Figure 4**); the results in terms of surface subsidence above each reservoir are shown in **Figure 5**, accounting for linear elasticity and unconventional elasto-plasticity as well. The effect of interaction among the different reservoirs can be seen from the shifting in time of the maximum value of subsidence as compared with the minimum of reservoir pressure: this phenomenon is also to be partly ascribed to the presence of clay layers confining the pools, but it is particularly evident when plasticity is introduced: as an extreme situation, maximum subsidence can not be reached even after 30 years; a "residual" delayed land subsidence has clearly appeared, so confirming the usefulness of the proposed unconventional plasticity model for modelling continuing surface settlements when reservoir pore pressures stabilize and for additional settlements

occurring even after the end of gas production.

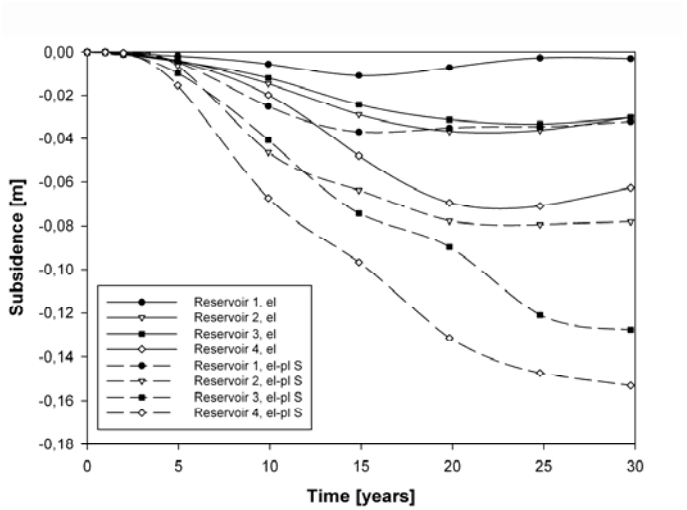

Figure 5: History of surface subsidence above the reservoirs.

The subsidence bowl is depicted in **Figure 6** and **Figure 7**, referring to the evolution of surface subsidence of Section A-A, **Figure 3**; apart from repeating the general trend shown in **Figure 5**, they evidence a subsidence bowl which appears, independently on time, to be slightly wider when elasto-plasticity is accounted for. It is to be underlined that the time scales involved, as well as the orders of magnitude for the resulting subsidence, agree well with what evidenced by [28] and [30] (the latter referring to linear elasticity only), with similar (or equal, as in the latter case) cumulative gas production histories and geological/geomechanical subsoil configurations.

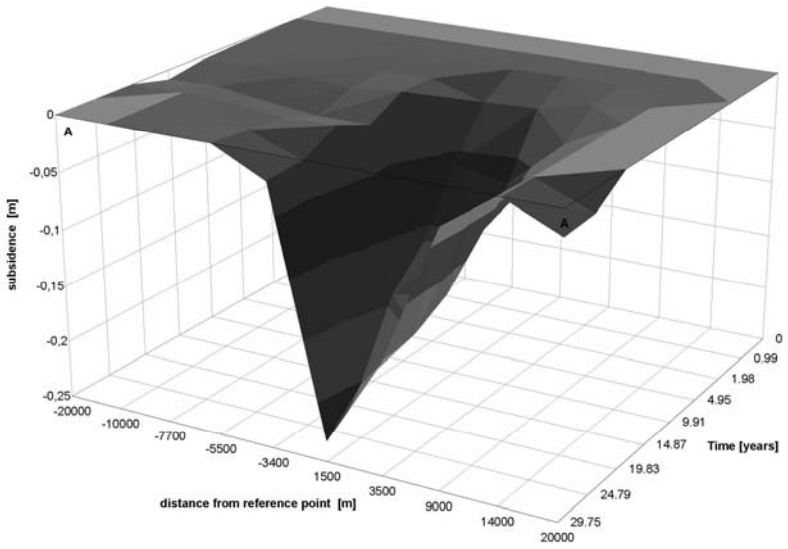

Figure 6: Subsidence bowl, linear elastic case.

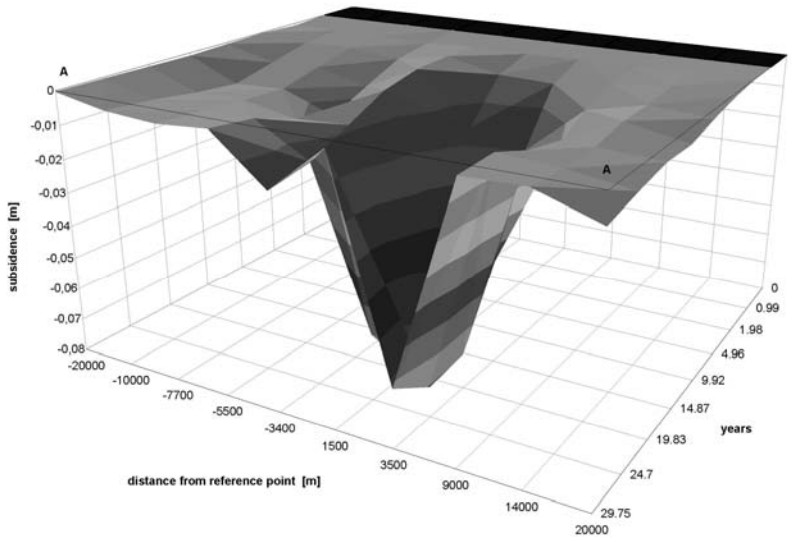

Figure 7: History of surface subsidence above the reservoirs.

5 CONCLUSIONS

The coupled hydro-mechanical state in soils coming from consolidation/subsidence processes and undergoing plasticity phenomena has been evaluated by means of the subloading surface model, allowing for predicting a smooth response for smooth monotonic loading, considering the sign of $\mathrm{tr}(\overline{\mathbf{N}}\mathbf{E}\mathbf{D})$ only in the loading criterion, automatically drawing back of a stress to the normal yield surface even if it goes out from the surface itself. Hence a rough numerical calculation with a large loading step is allowed and return-mapping iterative techniques can subsequently be skipped, so enhancing speedup and efficiency of large scale coupled analyses, as required when modelling subsidence in 3D domains and for long-term scenarios. The plasticity algorithm has been implemented in the PLASCON3D FE code, coupling hydro-thermo-mechanical fields within a saturated (locally partially saturated) porous medium subjected to external loads and water/gas withdrawals from deep layers (aquifers/reservoirs).

The plastic deformation due to the change of stress inside the yield surface exhibiting a smooth elastic-plastic transition has been described, as well as a first ability of describing softening behaviours has been shown.

Regional subsidence analyses due to gas extractions have been possible with reduced computational efforts when introducing unconventional elasto-plasticity in the code. It has been demonstrated that the time scales involved, as well as the orders of magnitude for the resulting subsidence, agree well with what evidenced by [28] and [30] (the latter referring to linear elasticity only), with similar (or equal, as in the latter case) cumulative gas production histories and geological/geomechanical subsoil configurations. Particularly, the effects of interaction among exploitations have been estimated, as well as the phenomenon of residual land subsidence near abandoned gas fields has been successfully modelled: the estimation of this delayed environmental cost of gas pumping is generally neglected, whereas it clearly

appears of being fundamental for an increased awareness of the consequence that gas production may have on future coastline stability relatively far from the gas field [28].

REFERENCES

[1] Poland J. (Ed.). *Guidebook to Studies of Land Subsidence due to Groundwater withdrawal*. UNESCO, Paris (1984).

[2] Terzaghi K. Die Berechnung der Durchlassigkeitsziffer des Tones aus dem Verlauf der hydrodynamischen Spannungserscheinungen. *Akademie der Wissenchaften in Wien, Sitzungsberichte, Mathematisch-naturwissenschaftliche Klasse*, Part Iia (1923) **132**(3/4): 125-138.

[3] Schrefler BA, Bolzon G, Salomoni V, Simoni L. On compaction in gas reservoirs. *Atti dell'Accademia Nazionale dei Lincei - Rendiconti Lincei: Scienze Fisiche e Naturali*, s. IX (1997) **VIII**(4): 235-248.

[4] Simoni L, Salomoni V, Schrefler BA. Elastoplastic subsidence models with and without capillary effects. *Comp. Meth. Appl. Mech. Engrg*. (1999) **171**(3-4): 491-502.

[5] Menin A, Salomoni VA, Santagiuliana R, Simoni L, Gens A, Schrefler BA. A mechanism contributing to subsidence above gas reservoirs. *Int. J. Comp. Meth. Engrg. Sci. Mech*. (2008) **9**(5): 270-287.

[6] Drucker DC. Conventional and unconventional plastic response and representation. *J. Appl. Mech. Rev.* ASME (1988) **41**(4):151-167.

[7] Hashiguchi K, Ueno M. Elastoplastic constitutive laws of granular materials. *Proceedings 9th Int. Conf. Soil Mech. Found. Engrg*., Special Session 9, Tokyo, Japan (1977): 73-82.

[8] Hashiguchi K. Constitutive equations of elastoplastic materials with elastic-plastic transitions. *J. Appl. Mech*. ASME (1980) **47**(2): 266-272.

[9] Hashiguchi K. Subloading surface model in unconventional plasticity. *Int. J. Solids Struct.* (1989) **25**(8): 917-945.

[10] Hashiguchi K, Saitoh K, Okayasu T, Tsutsumi S. Evaluation of typical conventional and unconventional plasticity models for prediction of softening behaviour of soils. *Geotech*. (2002) **52**(8): 561-578.

[11] Hashiguchi K. *Elastoplasticity theory*. In: F Pfeiffer, P Wriggers (Eds.), Lecture notes in applied and computational mechanics. Springer: Berlin (2009) **42**: 393 p.

[12] Yale DP. Coupled geomechanics-fluid flow modelling: effects of plasticity and permeability alteration. *SPE/ISRM Rock Mechanics Conference*. Irving, TX, USA, October 20-23 (2002) **SPE/ISRM 78202**: 10 p.

[13] Salomoni V.A., Fincato R. 3D subsidence analyses above gas reservoirs accounting for an unconventional plasticity model. *Int. J. Num. Anal. Meth. Geomech*. (2011) (in press).

[14] Lewis RW, Schrefler BA. *A finite element simulation of the subsidence of gas reservoirs undergoing a waterdrive*. In: RH Gallagher, DH Norrie, JT Oden, OC Zienkiewicz (Eds.), Finite Element in Fluids. Wiley: Chichester (1982) **4**: 179-199.

[15] Schrefler BA, Lewis RW, Majorana CE. Subsidence above volumetric and waterdrive gas reservoirs. *Int. J. Num. Meth. Fluids* (1981) **1**(2): 101-15.

[16] Lewis RW, Schrefler BA. *The finite element method in the deformation and consolidation of porous media*. Wiley: Chichester (1987).

[17] Lewis RW, Schrefler BA. *The finite element method in the static and dynamic*

deformation and consolidation of porous media. Wiley: Chichester (1998).
[18] Schrefler BA, Wang X, Salomoni V, Zuccolo G. An efficient parallel algorithm for three-dimensional analysis of subsidence above gas reservoirs. *Int. J. Num. Meth. Fluids* (1999) **31**(1): 247-60.
[19] Ferronato M, Gambolati G, Teatini P. On the role of reservoir geometry in waterdrive hydrodynamics. *J. Pet. Sci. Engrg.* (2004) **44**: 205-221.
[20] Hashiguchi K. Mechanical requirements and structures of cyclic plasticity models. *Int. J. Plasticity* (1993) **9**(6): 721-748.
[21] Hashiguchi K. The extended flow rule in plasticity. *Int. J. Plasticity* (1997) **13**(1): 37-58.
[22] Hashiguchi K. Fundamentals in constitutive equation: continuity and smoothness conditions and loading criterion. *Soils Found*. (2000) **40**(3): 155-161.
[23] Hashiguchi K. On the loading criterion. *Int. J. Plasticity* (1994) **10**(8): 871-878.
[24] Carbognin L, Gatto P, Mozzi G, Gambolati G. *Land subsidence of Ravenna and its similarities with the Venice case*. In: SK Saxena (Ed.), Evaluation and Prediction of Subsidence. ASCE: NY, USA (1978): 254-266.
[25] Gambolati G, Ricceri G, Bertoni W, Brighenti G, Vuillermin E. Mathematical simulation of the subsidence of Ravenna. *Water Res. Research* (1991) **27**(11): 2899-2918.
[26] Comerlati A, Ferronato M, Gambolati G, Putti M, Teatini P. Fluid-dynamic and geomechanical effects of CO_2 sequestration below the Venice Lagoon. *Env. Engrg. Geosc.* (2003) **XII**(3): 211-226.
[27] Schlumberger-GeoQuest. *Eclipse Simulator.* Version 2003A. Technical Description, Houston, TX, USA (2003).
[28] Baù D, Gambolati G, Teatini P. Residual land subsidence near abandoned gas fields raises concern over Northern Adriatic coastland. *Eos* (2000) **81**(22): 245-249.
[29] *Il Sole 24 Ore*. July 16 (2008) **195** (in Italian).
[30] AGIP. *Progetto Alto Adriatico – Studio di impatto ambientale*. AGIP, San Donato, Italy (1996) (in Italian).